0026-895X/05/6706-2137–2147$20.00
MOLECULAR PHARMACOLOGY
Vol. 67, No. 6

9225/3035864
Mol Pharmacol 67:2137–2147, 2005
Printed in U.S.A.

Expression, Pharmacological Profile, and Functional Coupling of A_{2B} Receptors in a Recombinant System and in Peripheral Blood Cells Using a Novel Selective Antagonist Radioligand, [^{3}H]MRE 2029-F20

Stefania Gessi, Katia Varani, Stefania Merighi, Elena Cattabriga, Cecilia Pancaldi, Youri Szabadkai, Rosario Rizzuto, Karl-Norbert Klotz, Edward Leung, Stephen Mac Lennan, Pier Giovanni Baraldi, and Pier Andrea Borea

Department of Clinical and Experimental Medicine, Pharmacology Unit (S.G., K.V., S.M., E.C., C.P., P.A.B.), Department of Diagnostic and Experimental Medicine, General Pathology Unit (R.R., Y.S.), and Department of Pharmaceutical Sciences (P.G.B.), University of Ferrara, Italy; Centro Nazionale di Eccellenza per lo Sviluppo di Metodologie Innovative per lo Studio ed il Trattamento delle Patologie Infiammatorie, Ferrara, Italy (S.G., K.V., S.M., E.C., C.P., P.A.B., R.R., Y.S.); Institut für Pharmakologie, Universitat Würzburg, Würzburg, Germany (K.N.K.); and King Pharmaceutical, Cary, North Carolina (E.L., S.M.)

Received December 6, 2004; accepted March 22, 2005

ABSTRACT

In this study, we compared the pharmacological and biochemical characteristics of A_{2B} adenosine receptors in recombinant (hA_{2B}HEK293 cells) and native cells (neutrophils, lymphocytes) by using a new potent 8-pyrazole xanthine derivative, [^{3}H]*N*-benzo[1,3]dioxol-5-yl-2-[5-(1,3-dipropyl-2,6-dioxo-2,3,6,7-tetrahydro-1*H*-purin-8-yl)-1-methyl-1*H*-pyrazol-3-yl-oxy]-acetamide] ([^{3}H]MRE 2029-F20), that has high affinity and selectivity for hA_{2B} versus hA_1, hA_{2A}, and hA_3 subtypes. [^{3}H]MRE 2029-F20 bound specifically to the hA_{2B} receptor stably transfected in human embryonic kidney (HEK) 293 cells with K_D of 2.8 ± 0.2 nM and B_{max} of 450 ± 42 fmol/mg of protein. Saturation experiments of [^{3}H]MRE 2029-F20 binding in human neutrophils and lymphocytes detected a single high-affinity binding site with K_D values of 2.4 ± 0.5 and 2.7 ± 0.7 nM, respectively, and B_{max} values of 79 ± 10 and 54 ± 8 fmol/mg of protein, respectively, in agreement with real-time reverse transcription polymerase chain reaction studies showing the presence of A_{2B} mRNA. The rank order of potency of typical adenosine ligands with recombinant hA_{2B} receptors was consistent with that typically found for interactions with the A_{2B} subtype and was also similar in peripheral blood cells. 5′-*N*-Ethylcarboxamidoadenosine stimulated cAMP accumulation in both hA_{2B}HEK293 and native cells, whereas phospholipase C activation was observed in recombinant receptors and endogenous subtypes expressed in neutrophils but not in lymphocytes. MRE 2029-F20 was revealed to be a potent antagonist in counteracting the agonist effect in both signal transduction pathways. In conclusion, [^{3}H]MRE 2029-F20 is a selective and high-affinity radioligand for the hA_{2B} adenosine subtype and may be used to quantify A_{2B} endogenous receptors. In this work, we demonstrated their presence and functional coupling in neutrophils and lymphocytes that play a role in inflammatory processes in which A_{2B} receptors may be involved.

Adenosine is a ubiquitous modulator that exerts its physiological functions through the interaction with four G protein-coupled receptors classified as A_1, A_{2A}, A_{2B}, and A_3

Article, publication date, and citation information can be found at http://molpharm.aspetjournals.org.
doi:10.1124/mol.104.009225.

ABBREVIATIONS: RT, reverse transcription; PCR, polymerase chain reaction; CGS 21680 2-[*p*-(2-carboxyethyl)-phenetylamino]-5′-*N*-ethylcarboxamidoadenosine; DPCPX, 8-cyclopentyl-1,3-dipropylxanthine; ZM 241385, (4-(2-[7-amino-2-(2-furyl)-[1,2,4]triazolo-[2,32][1,3,6]triazinyl-amino] ethyl)-phenol); MRS 1754, 8-[4[((4-cyano-[2,6]-phenyl)carbamoylmethyl)oxy)phenyl]-1,3-di(*n*-propyl)xanthine; OSIP339391, *N*-(2-{2-phenyl-6-[4-(3-phenylpropyl)-piperazine-1-carbonyl]-7*H*-pyrrolo[2,3-*d*]pyrimidin-4-ylamino}-ethyl)-acetamide; HEK, human embryonic kidney; MRE 3008-F20, 5-*N*-(4-methoxyphenyl-carbamoyl)amino-8-propyl-2(2furyl)-pyrazolo-[4,3e-1,2,4-triazolo [1,5-*c*] pyrimidine; MRE 2029-F20, *N*-benzo[1,3]dioxol-5-yl-2-[5-(1,3-dipropyl-2,6-dioxo-2,3,6,7-tetrahydro-1*H*-purin-8-yl)-1-methyl-1*H*-pyrazol-3-yl-oxy]-acetamide]; Ins(1,4,5)P_3, inositol 1,4,5-trisphosphate; CHA, N^6-cyclohexyladenosine; NECA, 5′-*N*-ethyl-carboxamidoadenosine; (*R*)-PIA, *R*(−)-N^{6}-(2-phenyl-isopropyl)-adenosine; (*S*)-PIA, *S*(−)-N^{6}-(2-phenylisopropyl)adenosine; IB-MECA, N^6-(3-iodobenzyl) adenosine-5′-*N*-methyluronamide; CGS 15943, 5-amino-9-chloro-2-(furyl)1,2,4-triazolo[1,5-*c*] quinazoline; AS 16, 2-(4-benzyloxy-phenyl)-*N*-[5-(2,6-dioxo-1,3-dipropyl-2,3,6,7-tetrahydro-1*H*-purin-8-yl)-1-methyl-1*H*-pyrazol-3-yl-oxy]-acetamide]; AS 100, *N*-2,3,4 dichlorophenyl)-2-[5-(2,6-dioxo-1,3-dipropyl-2,3,6,7-tetrahydro-1*H*-purin-8-yl)-1-methyl-1*H*-pyrazol-3-yl-oxy]-acetamide]; Ct, cycle threshold; KRPG, Krebs-Ringer phosphate buffer; SCH 58261, 7-(2-phenylethyl)-2-(2-furyl)-pyrazolo[4,3-*e*]-1,2,4-triazolo[1,5-*c*]-pyrimidine; IP_3, inositol trisphosphate; PLC, phospholipase C; hA_{2B}HEK 293 cells, human embryonic kidney-293 cells transfected with human adenosine A_{2B} receptor; fMLF, *N*-formyl-L-methionyl-L-leucyl-L-phenylalanine; U73122, 1-[6-([(17*β*)-3-methoxyestra-1,3,5(10)-trien-17-yl]amino)hexyl]-1*H*-pyrrole-2,5-dione.

(Fredholm et al., 2001; Fredholm, 2003). In particular, A_{2B} receptors are associated with stimulation of the adenylate cyclase and activation of phospholipase C through the coupling to Gs and $G_{q/11}$ proteins, respectively. A_{2B} receptors have been found on practically every cell in most species. RT-PCR studies revealed their highest expression in cecum, large intestine, and urinary bladder, but lower levels in brain, spinal cord, lung, and vas deferens (Rivkees and Reppert, 1992). However, besides regulation at the level of gene expression, targeting of the receptor protein to specific cells or tissues is crucial in understanding their role in pathophysiological conditions. The lack of selective pharmacological tools has hampered research in this field; in particular, the lack of selective A_{2B} receptor agonists has undoubtedly contributed to the general lack of information of their physiological functions. The characterization of A_{2B} receptors, therefore, often relies on the lack of effectiveness of compounds that are potent and selective agonists of other receptor subtypes. The agonist CGS 21680, for example, has been useful in differentiating between A_{2A} and A_{2B} receptors (Feoktistov and Biaggioni, 1995; Fiebich et al., 1996, 1997). However, pharmacological characterization of receptors based on apparent agonist potencies is far from ideal, because it depends not only on agonist binding to the receptor but also on multiple processes involved in signal transduction (Feoktistov et al., 2001). Based on functional assays using novel A_{2B} selective antagonists, significant progress has been made in the understanding of the molecular pharmacology and physiology of A_{2B} adenosine receptors. They seem to be implicated in mast-cell secretion (Feoktistov et al., 2001), coronary flow regulation (Talukder et al., 2003), neoangiogenesis (Grant et al., 2001; Feoktistov et al., 2002, 2003; Afzal et al., 2003), cytokine release by bronchial smooth muscle cells (Zhong et al., 2004), and nociception (Abo-Salem et al., 2004), suggesting a possible role of the A_{2B} subtype in the modulation of inflammatory processes involved in asthma, tumor growth, tissue injury, ischemia, and pain (Feoktistov et al., 2003; Livingston et al., 2004).

The characterization of A_{2B} receptors through radioligand binding studies has been performed, until now, by using low-affinity and nonselective antagonists, such as [^{3}H]-DPCPX, [^{3}H]ZM 241385, and 3-(3-[^{125}I]iodo-4-aminobenzyl)-8-(4-oxyacetate)phenyl-1-propylxanthine, that, as a consequence of their low affinity, display a rapid dissociation rate from the receptor. In addition, because these ligands are nonselective, their utility in native systems is hampered because many tissues and cell lines express several adenosine subtypes. Based on these considerations, it is evident that, to obtain more information about the physiological role of A_{2B} receptors, new radiolabeled compounds with high affinity and selectivity should be synthesized. High-affinity radioligands for A_{2B} receptors, [^{3}H]MRS 1754, and [^{3}H]-OSIP339391 have been introduced (Ji et al., 2001; Stewart et al., 2004), but they were not commercially available at the time of this study. Our group has identified a series of 8-pyrazole xanthine derivatives as potent and selective human A_{2B} adenosine antagonists (Baraldi et al., 2004a,b), and a radiolabeled form of one compound of this series was used as a new pharmacological tool to describe the comparison between human recombinant A_{2B} receptors stably transfected in HEK 293 cells (hA_{2B}HEK 293 cells) and endogenous receptors present in neutrophils and lymphocytes, which represent inflammatory cells potentially involved in the exacerbation of asthma and other inflammatory processes in which A_{2B} receptors are thought to be involved. In this study, we demonstrated that A_{2B} receptors are strongly linked to adenylyl cyclase in both transfected and native cells, whereas for phospholipase C activity, they are well coupled in transfected cells, less in neutrophils, and not at all in lymphocytes, where the A_{2B} expression is quite low.

Materials and Methods

Materials. [^{3}H]MRE 2029-F20 (specific activity, 123 Ci/mmol) and [^{3}H]MRE 3008-F20 (specific activity, 67 Ci/mmol) were synthesized at Amersham Biosciences (Little Chalfont, Buckinghamshire, UK); [^{3}H]ZM 241385 (specific activity, 20 Ci/mmol) was purchased from Tocris (Boston, MA). [^{3}H]DPCPX (specific activity, 120 Ci/mmol) and [^{3}H]Ins(1,4,5)P_3 (specific activity, 21 Ci/mmol) were obtained from PerkinElmer Life and Analytical Sciences (Boston, MA). CHA, NECA, (*R*)-PIA, (*S*)-PIA, CGS 21680, IB-MECA, CGS 15943, and DPCPX were obtained from Sigma/RBI (Natick, MA). MRS 1754 was obtained from Sigma-Aldrich (Milano, Italy). SCH 58261, MRE 3008-F20, MRE 2029-F20, AS 16, and AS 100 were synthesized by Prof. P. G. Baraldi (Department of Pharmaceutical Sciences, University of Ferrara, Ferrara, Italy). All other reagents were of analytical grade and obtained from commercial sources.

Synthesis of [^{3}H]MRE 2029-F20. The synthesis of [^{3}H]MRE 2029-F20 was prepared through custom synthesis at Amersham Bioscience from tritium gas by a method developed by Nycomed Amersham plc. The product was purified by reversed-phase high-performance liquid chromatography using an acetonitrile/trifluoroacetic acid gradient (Baraldi et al., 2004a).

Stable Transfection of HEK 293 Cells. cDNA encoding human A_{2B} receptors was a gift of Prof. Karl-Norbert Klotz (Institut für Pharmakologie und Toxikologie, Universitat Würzburg, Würzburg, Germany) and subcloned into the expression plasmid pcDNA 3.1 (Invitrogen). The plasmid was amplified into a competent *Escherichia coli* strain and plasmid DNA isolated by using QIAGEN Maxiprep columns (plasmid purification kit; QIAGEN, Valencia, CA). cDNA was then sequenced on both strands in the University of Padova, DNA Sequence Service CRIBI, and transfected into HEK 293 cells by using the calcium phosphate precipitation method (Chen and Okayama, 1987). Colonies were selected by growth of cells on 0.8 mg/ml G-418. Stably transfected cells were maintained in Dulbecco's modified Eagle's medium/Ham's F-12 medium (Dulbecco's modified Eagle's medium/F-12 medium) with 10% fetal calf serum, 100 U/ml penicillin, 100 mg/ml streptomycin, and 0.3 mg/ml G-418, at 37° in 5% CO_2/95% air.

Membrane Preparation. For membrane preparation, the culture medium was removed. The cells were washed with phosphate-buffered saline and scraped off T75 flasks in ice-cold hypotonic buffer (5 mM Tris HCl and 2 mM EDTA, pH 7.4). The cell suspension was homogenized using a Polytron homogenizer, and the homogenate was spun for 30 min at 36,000*g*. The membrane pellet was resuspended in 50 mM Tris-HCl buffer, containing 10 mM $MgCl_2$, 1 mM EDTA, and 0.1 mM benzamidine, pH 7.4, and incubated with 2 IU/ml adenosine deaminase for 30 min at 37°C. The protein concentration was determined according to a Bio-Rad method (Bradford, 1976) with bovine serum albumin as reference standard.

Peripheral Blood Cells Isolation. Lymphocytes and neutrophils were isolated from buffy coats kindly provided by the Blood Bank of the University Hospital of Ferrara, according to Gessi et al. (2002, 2004). In brief, the blood was centrifuged on Ficoll-Hypaque density gradients. The human peripheral blood mononuclear cells were isolated and removed from the Ficoll-Hypaque gradients. Thereafter, they were washed in 0.02 M phosphate-buffered saline at pH 7.2. Further purification of lymphocytes from peripheral blood mononuclear cells was performed by adhesion of monocytes to plastic plates for 2 h at 37°C. To obtain neutrophils, the lower phase of Ficoll-Hypaque gradients was washed and supplemented with 20 ml of 6% Dextran T500. After gentle mixing, erythrocytes were allowed to settle at 20°C for 60 min. The remaining erythrocytes were lysed by suspending the cell pellet in 10 ml of distilled water at 4°C under gentle agitation. After 30 s, isotonicity was restored by adding 3 ml of a solution containing 0.6 M NaCl. Neutrophils were sedimented by centrifugation at 20°C for 20 min at 250*g*. This procedure resulted in approximately 95% neutrophils, and the cell viability was more than 95% as detected by trypan blue exclusion test. Rat neutrophils and lymphocytes were isolated from male Sprague-Dawley rats (300−350 g; Stefano Morini, Reggio Emilia, Italy). Blood samples from the inferior vena cava were collected in an EDTA-anticoagulated tube, diluted in phosphate-buffered saline, and isolated by density gradient centrifugation (Ficoll-Hypaque) as described above for human blood cells. Membrane preparations were performed essentially according to Gessi et al. (2002; 2004).

Real-Time RT-PCR Experiments. Total cytoplasmic RNA was extracted from HEK 293 and peripheral blood cells by the acid-guanidinium-thiocyanate-phenol method (Chomczynski and Sacchi, 1987). Quantitative real-time RT-PCR assay (Higuchi et al., 1993) of A_{2B} mRNA transcript was carried out using gene-specific double fluorescently labeled TaqMan MGB probe (minor groove binder) in an ABI Prism 7700 Sequence Detection System (Applied Biosystems, Warrington Cheshire, UK). For the real-time RT-PCR of the A_{2B} gene, the assays-on-demand gene expression product (GenBank accession no. NM_0006756) was used with the fluorescent reporter 6-carboxy fluorescein and the quencher 6-carboxy-*N*,*N*,*N*′,*N*′-tetramethylrhodamine. For the real-time RT-PCR of the reference gene, the endogenous control human β-actin kits was used, and the probe was fluorescence-labeled with VIC (Applied Biosystems, Monza, Italy). Moreover, a curve of A_{2B} cDNA plasmid standards with a range spanning at least 6 orders of magnitude (10^{-11}–10^{-16} g/μl) was generated. This standard curve displayed a linear relationship between Ct values and the logarithm of plasmid amount. Therefore, quantification of A_{2B} message in blood cells was made by interpolation from standard curve of Ct values generated from the plasmid dilution series.

Binding Assays to Human Cloned Adenosine Receptors. Binding assays to human cloned A_1, A_{2A}, and A_3 receptors were performed at 4°C using [^{3}H]DPCPX, [^{3}H]ZM 241385, and [^{3}H]MRE 3008-F20, respectively, as described by Varani et al. (2000).

[^{3}H]MRE 2029-F20 Binding Assays. Kinetic studies of [^{3}H]MRE 2029-F20 (2.5 nM) were performed incubating membranes obtained by HEK 293 cells transfected with the human A_{2B} receptors in a thermostatic bath at 4°C. A total assay volume of 250 μl was employed in which the final protein level was 70 μg per well. For the measurement of the association rate, the reaction was terminated at different times (from 5 to 180 min) by rapid filtration under vacuum, followed by washing with 5 ml of ice-cold buffer four times. For the measurement of dissociation rate, the samples were incubated at 4° for 90 min, and then 1 μM MRE 2029-F20 was added to the mixture. The reaction was terminated at different times from 5 to 100 min. Saturation binding experiments of [^{3}H]MRE 2029-F20 (0.3 to 30 nM) to hA_{2B} HEK293 cell membranes were performed by incubation for 90 min at 4°C. Competition experiments of 3 nM [^{3}H]MRE 2029-F20 were performed in duplicate in a final volume of 250 μl in test tubes containing 50 mM Tris HCl buffer, 10 mM $MgCl_2$, 1 mM EDTA, and 0.1 mM benzamidine, pH 7.4, 100 μl of membranes, and at least 12 to 14 different concentrations of typical adenosine receptor agonists and antagonists. Nonspecific binding was defined as binding in the presence of 1 μM MRE 2029-F20 and, at the K_D value of the radioligand, was approximately 30 to 35% and 40 to 45% of total binding in HEK 293 cells and in blood cells, respectively. Similar results were obtained in the presence of 10 μM DPCPX and 100 μM NECA. Bound and free radioactivity were separated by filtering the assay mixture through Whatman GF/B glass-fiber filters using a Micro-Mate 196 cell harvester (PerkinElmer Life and Analytical Sciences). The filter bound radioactivity was counted with a Top Count microplate scintillation counter (efficiency, 57%) with MicroScint 20. K_i values were calculated from IC_{50} values according to the Cheng and Prusoff equation, $K_i = IC_{50}/(1 + [C^*]/K_D^*)$, where $[C^*]$ is the concentration of the radioligand and K_D^* is its dissociation constant. A weighted nonlinear least-squares, curve-fitting program LIGAND (Munson and Rodbard, 1980) was used for computer analysis of saturation and inhibition experiments.

Cyclic AMP Assay. hA_{2B}HEK-293 and peripheral blood cells were suspended in 0.5 ml of Krebs-Ringer phosphate buffer (KRPG) (136 mM NaCl, 5 mM KCl, 0.67 mM Na_2HPO_4, 0.2 mM KH_2PO_4, 3 mM $NaHCO_3$, 1 mM $CaCl_2$, 5 mM glucose, 5 mM HEPES, 10 mM $MgCl_2$, and 2.0 IU/ml adenosine deaminase, pH 7.4) containing 0.5 mM 4-(3-butoxy-4-methoxybenzyl)-2-imidazolidinone (Ro 20-1724) as phosphodiesterase inhibitor, and preincubated for 10 min in a shaking bath at 37°C. Then the nonselective adenosine agonist NECA was added to the mixture, and the incubation continued for a further 10 min. The reaction was terminated by the addition of ice-cold 6% trichloroacetic acid. The trichloroacetic acid suspension was centrifuged at 2000*g* for 10 min at 4°C, and the supernatant was extracted four times with water-saturated diethyl ether. The final aqueous solution was tested for cyclic AMP levels by a competition binding assay carried out essentially according to Varani et al. (1997). Samples of cyclic AMP standards (0–10 pmol) were added to each test tube containing the incubation buffer (0.1 M Trizma base, 8.0 mM aminophylline, and 6.0 mM 2-mercaptoetanol, pH 7.4) and [^{3}H]cyclic AMP in a total volume of 0.5 ml. The binding protein, previously prepared from beef adrenal glands, was added to the samples and incubated at 4° for 150 min. After the addition of charcoal, samples were centrifuged at 2000*g* for 10 min. The clear supernatant (0.2 ml) was mixed with 4 ml of Atomlight and counted in a LS-1800 Beckman scintillation counter.

Ins(1,4,5)P_3 Binding Assay. IP_3 generation in hA_{2B}HEK 293 and peripheral blood cells was measured by [^{3}H]Ins(1,4,5)P_3 competition assay to IP_3 binding protein according to the method described by Challiss et al. (1990). hA_{2B}HEK 293 cells (2×10^6 cells in each tube) and peripheral blood cells (8×10^6 cells in each tube) were suspended in KRPG buffer and stimulated with agonists at 37°C. The reaction was terminated by addition of 0.5 M trichloroacetic acid. Acidified samples were left on ice for 15 min, centrifuged at 3000*g* for 15 min at 4°C and trichloroacetic acid was extracted with five 2-vol washes with water-saturated diethyl ether. Finally, 125 μl of 30 mM EDTA and 125 μl of 60 mM $NaHCO_3$ were added to 500 μl of cell extract, and samples were taken for analysis. Buffer samples were also taken through the acidification/extraction protocol to provide diluent for the Ins(1,4,5)P_3 assay standard curve. A 30-μl portion of sample or of trichloroacetic acid-extracted buffer containing standard amounts of Ins(1,4,5)P_3 (0.12–12 pmol) or DL-Ins(1,4,5)P_3 (0.3 nmol to define nonspecific binding) was added to 30 μl of assay buffer (25 mM Tris HCl and 1 mM EDTA, pH 8) and 30 μl of [^{3}H]Ins(1,4,5)P_3 (7000 dpm/assay). Then, 30 μl (0.4 mg of protein) of the adrenal-cortical binding protein preparation was added and incubation continued for 30 min. Bound and free [^{3}H]Ins(1,4,5)P_3 were separated by rapid filtration through Whatman GF/B glass fiber filters with four 3-ml washes of ice-cold 25 mM Tris HCl, 1 mM EDTA, and 5 mM $NaHCO_3$, pH 8. Scintillator was added to the filter discs, and radioactivity was determined after a 12-h extraction period by scintillation counting.

Measurement of Cytosolic Ca^{2+} Concentration. $[Ca^{2+}]_i$ was evaluated by incubating hA_{2B}HEK 293 cells with the Ca^{2+}-sensitive fluorescent dye Fura 2-acetoxymethyl ester (5 μM) in KRPG buffer for 45 min at 37°C. Alternate excitation at 340 nM and 380 nM was supplied, and the F_{340}/F_{380} emission ratio was recorded with a dynamic image analysis system (Laboratory Automation 2.0; RCS, Florence, Italy). For calcium measurements in human lymphocytes and neutrophils, cells were loaded with fura 2-acetoxymethyl ester (2 μM) in KRPG buffer, for 30 min at 37°C, according to Gessi et al. (2002). The cells were centrifuged at 1000*g* for 10 min to remove extracellular dye and were resuspended in KRPG solution at 4×10^6 cells/ml. Fluorescence was monitored with a LS50 spectrofluorometer (PerkinElmer Life and Analytical Sciences), at excitation wavelengths of 340 and 380 nm and an emission wavelength of 505 nm, in cuvettes thermostatically controlled at 37°C and continuously stirred.

Results

Real-Time RT-PCR Experiments. HEK 293 cells are recognized as cells expressing native A_{2B} receptors. Therefore, the mRNA presence of this adenosine subtype was investigated in both wild-type and hA_{2B}HEK 293 cells. Transfection of A_{2B} receptors in HEK 293 cells produced a 350 ± 30-fold increase of A_{2B} mRNA accumulation with respect to the corresponding wild-type cells; the expression level of A_{2B} receptors was normalized to the expression level of the endogenous reference (β-actin) in each sample (Fig. 1, A and B). In addition, the mRNA level of A_{2B} receptors was investigated in primary cells in which this adenosine subtype is supposed to play an important regulatory role, such as peripheral blood cells. The amount of product was expressed as the ratio of mRNA (determined by interpolation from standard curve of Ct values generated from the plasmid dilution series) and total RNA and indicated the following rank order: monocytes < lymphocytes ≈ neutrophils, with monocytes expressing approximately 4-fold less mRNA compared with the other blood cells (Student's t test; *, $P < 0.01$ versus monocytes) (Fig. 1C).

Radioligand Binding Studies in Recombinant and Native Cells. Fig. 2A shows that [^{3}H]MRE 2029-F20 binding to hA_{2B}HEK 293 cells reached equilibrium after approximately 45 min and was stable for at least 3 h. [^{3}H]MRE 2029-F20 binding was rapidly reversed by the addition of 1 μM MRE 2029-F20 as shown in Fig. 2B. A one-component model fit association and dissociation curves significantly better than a two-component model ($P < 0.05$). The rate constants were: $k_{obs} = 0.046 \pm 0.002$ min^{-1} and $k_{-1} = 0.025 \pm 0.003$ min^{-1}. From these values, a kinetic dissociation constant (K_D) of 2.98 nM was calculated. Figure 3 shows a saturation curve of [^{3}H]MRE 2029-F20 to adenosine A_{2B} receptor, and the linearity of the Scatchard plot in the inset is indicative, in our experimental conditions, of the presence of a single class of binding sites with a K_D value of 2.8 ± 0.2 nM and a B_{max} value of 450 ± 42 fmol/mg of protein. In contrast to the presence of mRNA message, no specific binding of [^{3}H]MRE 2029-F20 was detectable in HEK 293 wild-type cells (data not shown). Table 1 shows the affinities, expressed as K_i values, of selected adenosine receptor agonists and antagonists to hA_{2B} receptors expressed in HEK 293 cells using [^{3}H]MRE 2029-F20. The order of potency in [^{3}H]MRE 2029-F20 displacement assays for adenosine receptor agonists was NECA > (R)-PIA > CHA > IB-MECA > (S)-PIA > CGS 21680 (Fig. 4A). The order of potency of the receptor antagonists was: MRE 2029-F20 > MRS 1754 > AS 100 > ZM 241385 > CGS 15943 > AS 16 > DPCPX > enprofylline > theophylline (Fig. 4B). The selectivity of MRE 2029-F20 for the human A_{2B} over A_1, A_{2A}, and A_3 receptors was evaluated in radioligand binding assays by using [^{3}H]DPCPX, [^{3}H]ZM 241385, and [^{3}H]MRE 3008-F20, respectively. MRE 2029-F20 displays low affinity for the human A_1 receptor (K_i = 245 ± 31 nM) and no significant affinity for the human A_{2A} and A_3 subtypes (K_i > 1000 nM). This indicates that MRE 2029-F20 is 88-fold selective for A_{2B} over A_1 receptors and more than 300-fold selective for A_{2B} over A_{2A} and A_3 subtypes, which means a range of selectivity similar to [^{3}H]MRS 1754 (selectivity of 210-, 260-, and 290-fold for A_{2B} over A_1, A_{2A}, and A_3 subtypes, respectively) and

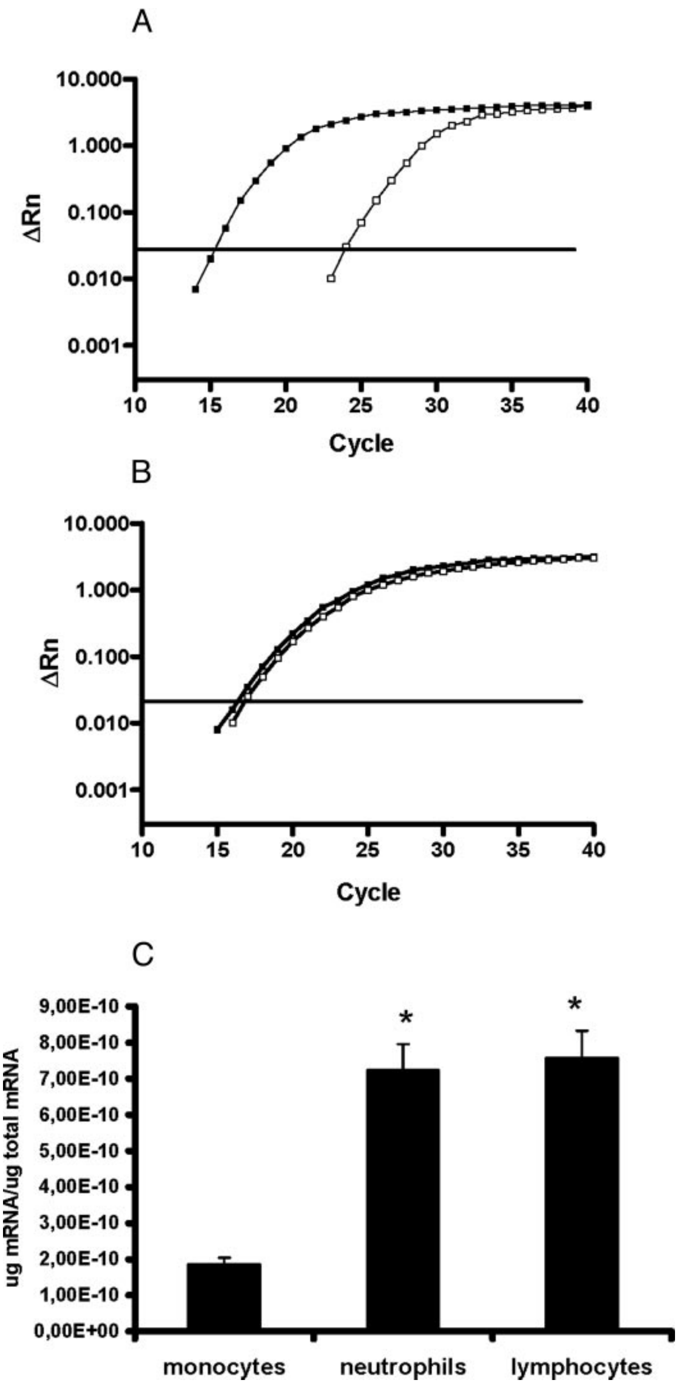

Fig. 1. Representative amplification plots for the A_{2B} receptors mRNA in transfected (■) and untransfected (□) HEK 293 cells (A) compared with the respective β -actin mRNA (B). C, expression of A_{2B} receptors mRNA in monocytes, lymphocytes, and neutrophils. The amount of product in blood cells was expressed as the ratio of mRNA (micrograms) determined by interpolation from standard curves of Ct values generated from the plasmid dilution series and total RNA (micrograms) used in retrotranscription reaction. Results are presented as the mean ± S.E.M. of four independent experiments (Student's t test; *, $P < 0.01$ versus monocytes).

better than [^{3}H]OSIP339391 (selectivity of 70-fold for A_{2B} over A_1, A_{2A}, and A_3 subtypes) (Ji et al., 2001; Stewart et al., 2004). Saturation experiments of [^{3}H]MRE 2029-F20 binding performed at 21 and 37°C revealed K_D values of 3.5 ± 0.4 and 6.5 ± 0.7 nM and B_{max} values of 460 ± 50 and 430 ± 48 fmol/mg of protein, respectively, thus suggesting that dissociation constants increased with temperature, whereas B_{max} data were largely independent of it. This binding behavior has previously been found to be typical of adenosine A_1, A_{2A}, and A_3 subtypes (Borea et al., 1996; Varani et al., 2000). To investigate whether MRE 2029-F20 would be a useful tool to detect A_{2B} receptors in primary cells, we isolated monocytes, lymphocytes, and neutrophils from peripheral blood. As for human monocytes, it was not possible to detect A_{2B} receptors, even though the mRNA was present, suggesting that possibly in these cells their level was extremely low. On the other hand, in agreement with real-time RT-PCR experiments, neutrophils and lymphocytes both express A_{2B} subtype with the following binding parameters: K_D of 2.4 ± 0.5 and 2.7 ± 0.7 nM and B_{max} of 79 ± 10 and 54 ± 8 fmol/mg of protein, respectively (Fig. 5, A and B). The pharmacological profile of selected adenosine agonists and antagonists obtained from inhibition binding experiments in peripheral blood cells revealed a rank order of potency strictly similar to that obtained in transfected cells: NECA > (*R*)-PIA > CHA> IB-MECA > (*S*)-PIA >CGS 21680 and MRE 2029-F20 > MRS 1754 > AS100 > ZM 241385 > AS16 > DPCPX > enprofylline > theophylline (Table 1). Specific binding of [^{3}H]MRS 2029-F20 (55–60%) was also detected in rat neutrophils and lymphocytes.

Evaluation of cAMP Levels. To investigate the functional coupling of native and recombinant A_{2B} receptors to adenylyl cyclase, we evaluated the stimulation of cAMP production in hA_{2B}HEK 293 cells and in peripheral blood cells. Our results show that in hA_{2B}HEK 293 cells, NECA showed a potency greater in cAMP (EC_{50} value of 4.5 ± 0.4 nM) than in radioligand binding studies (K_i value of 262 ± 30 nM) (Fig. 6A). We were surprised to find that this effect was not potently antagonized by MRE 2029-F20 that showed an IC_{50} value of 150 ± 18 nM. Because of the low potency of MRE 2029-F20 in inhibiting cAMP accumulation induced by NECA, we suspected the presence of basal levels of A_{2A} receptors in addition to A_{2B} in wild-type HEK 293 cells. This was assessed by real-time RT-PCR experiments revealing a similar amount of A_{2A} and A_{2B} mRNA expression (data not

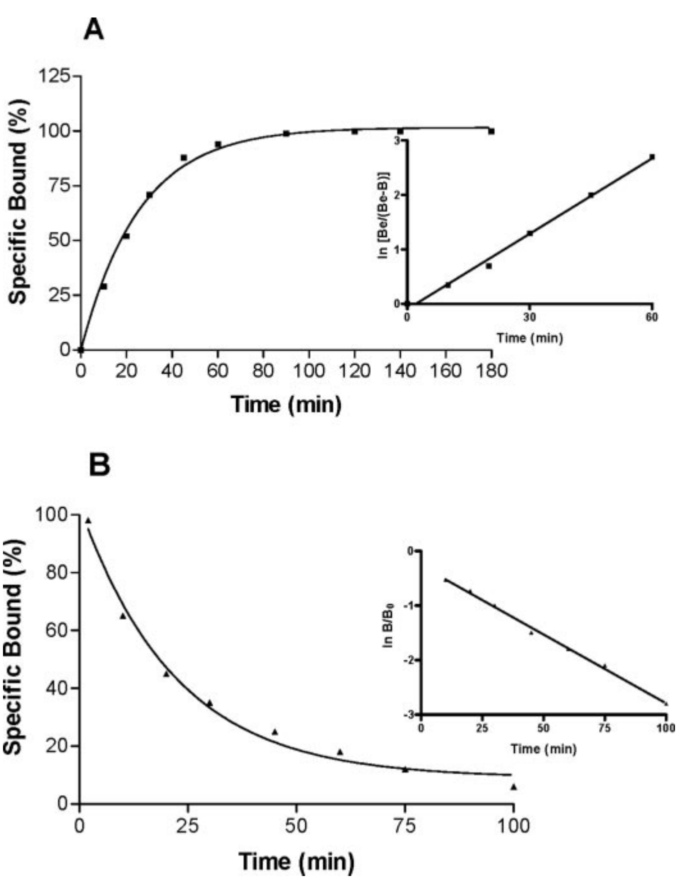

Fig. 2. A, kinetics of [^{3}H]MRE 2029-F20 binding to human A_{2B} adenosine receptors in HEK 293 cells, with association curves representative of a single experiment that was replicated three times with similar results. Inset, first-order plot of [^{3}H]MRE 2029-F20 binding. Be, amount of [^{3}H]MRE 2029-F20 bound at equilibrium; B, amount of [^{3}H]MRE 2029-F20 bound at each time. Association rate constant was: k_{+1} = 0.0084 ± 0.0009 min^{-1} nM^{-1}. B, kinetic of [^{3}H]MRE 2029-F20 binding to human A_{2B} adenosine receptors; dissociation curve represents a single experiment. Inset, first-order plot of [^{3}H]MRE 2029-F20 binding. Dissociation rate constant was: k_{-1} = 0.025 ± 0.003 min^{-1}.

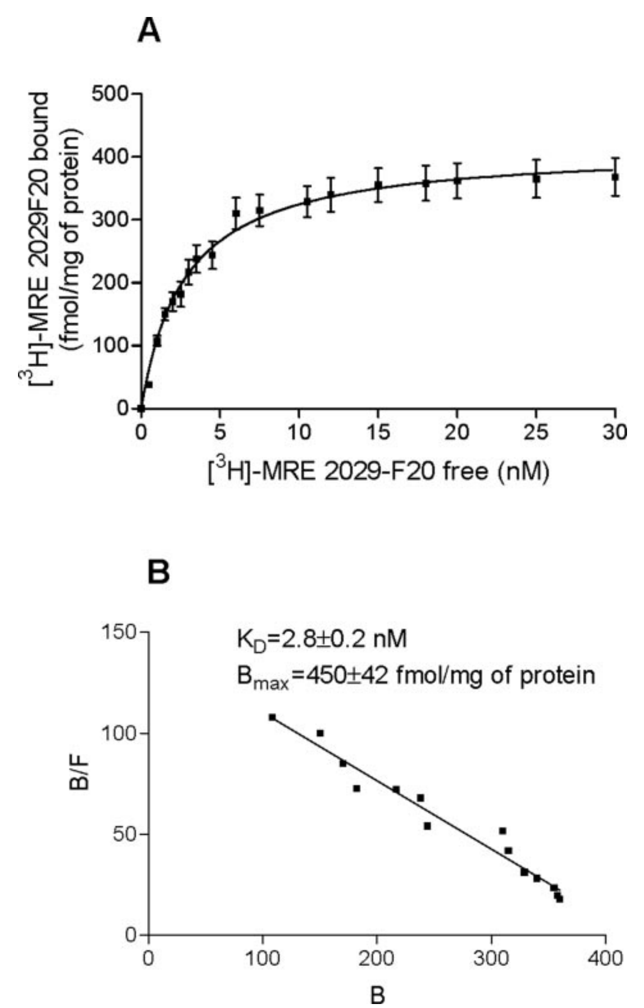

Fig. 3. A, saturation of [^{3}H]MRE 2029-F20 binding to A_{2B} adenosine receptors in HEK 293 cells. Data points are the means and vertical lines are the S.E.M. of four separate experiments performed in triplicate. B, Scatchard plot of the same data are shown. K_D value was 2.8 ± 0.2 and B_{max} value was 450 ± 42 fmol/mg of protein. Experiments were performed as described under *Materials and Methods*.

shown) and confirmed by saturation binding experiments of [^{3}H]ZM 241385 binding (0.1–10 nM) showing an affinity of 1.04 ± 0.2 nM and a density of 35 ± 4 fmol/mg of protein. This value was possibly not caused by a contaminating presence of endogenous A_{2B} receptors, as demonstrated by the lack of [^{3}H]MRE 2029-F20 specific binding in untransfected HEK 293 cells. CGS 21680, an A_{2A}-selective agonist, stimulated cAMP levels with an EC_{50} of 410 ± 52 nM, but it was less efficacious than NECA. The unstimulated level of cAMP was 15 ± 3 pmol/10^{6}cells; at concentrations producing maximal effects (10 μM), CGS 21680 induced a 4-fold increase, whereas NECA caused an 8-fold increase in cAMP (to 60 ± 8 and 120 ± 15 pmol/10^{6}cells, respectively), suggesting the activation, in the first case, of only A_{2A} receptors and, in the second, of both A_{2A} and A_{2B} subtypes (Fig. 6A). Therefore to evaluate the potency of MRE 2029-F20 at A_{2B} receptors, a Schild analysis of this compound was performed in the presence of the A_{2A} blocker, SCH 58261 (100 nM). The pA_2 value of MRE 2029-F20 was 7.81 ± 0.10 nM, in agreement with its affinity in binding experiments performed at 37°C (K_D = 6.5 ± 0.7 nM) (Fig. 6B). In human neutrophils and lymphocytes expressing different adenosine subtypes, the nonselective agonist NECA, through the activation of both A_{2A} and A_{2B} receptors, showed EC_{50} values of 147 ± 16 and 220 ± 20 nM, respectively. The unstimulated levels of cAMP were 20 ± 5 and 16 ± 4 pmol/10^{6}cells and were increased by NECA stimulation to 80 ± 15 and 60 ± 9 in neutrophils and lymphocytes, respectively. To distinguish the role played by the two stimulatory adenosine subtypes, we repeated the concentration-response curve of NECA in the presence of 100 nM

TABLE 1

K_i values from competition experiments with [^{3}H]MRE 2029-F20 of selected adenosine receptor agonists and antagonists for A_{2B} receptors in hA_{2B} HEK 293 cells, human neutrophils, and lymphocytes

Results are presented as the mean ± S.E.M. of four independent experiments.

	hA_{2B} HEK 293	Human Neutrophils	Human Lymphocytes
		nM	
Agonists			
NECA	262 ± 30	315 ± 37	340 ± 42
(*R*)-PIA	3500 ± 440	4800 ± 550	5300 ± 570
(*S*)-PIA	8500 ± 920	9200 ± 950	9700 ± 990
CHA	4200 ± 450	5100 ± 530	5600 ± 600
IB-MECA	7600 ± 800	8300 ± 870	9000 ± 980
CGS 21680	>10,000	>10,000	>10,000
Antagonists			
MRE 2029-F20	3.0 ± 0.15	3.5 ± 0.6	4.0 ± 0.7
MRS 1754	3.5 ± 0.20	4.6 ± 0.4	5.2 ± 0.5
AS 16	22 ± 1.5	35 ± 5	40 ± 6
AS 100	3.8 ± 0.31	5.0 ± 0.4	5.5 ± 0.8
CGS 15943	9.8 ± 0.9	N.T.	N.T.
ZM 241385	9.0 ± 0.8	22 ± 4	18 ± 2
DPCPX	35 ± 5	41 ± 5	45 ± 6
Enprofylline	5500 ± 600	6200 ± 700	6800 ± 750
Theophylline	6700 ± 800	7500 ± 800	7900 ± 900

N.T., not tested.

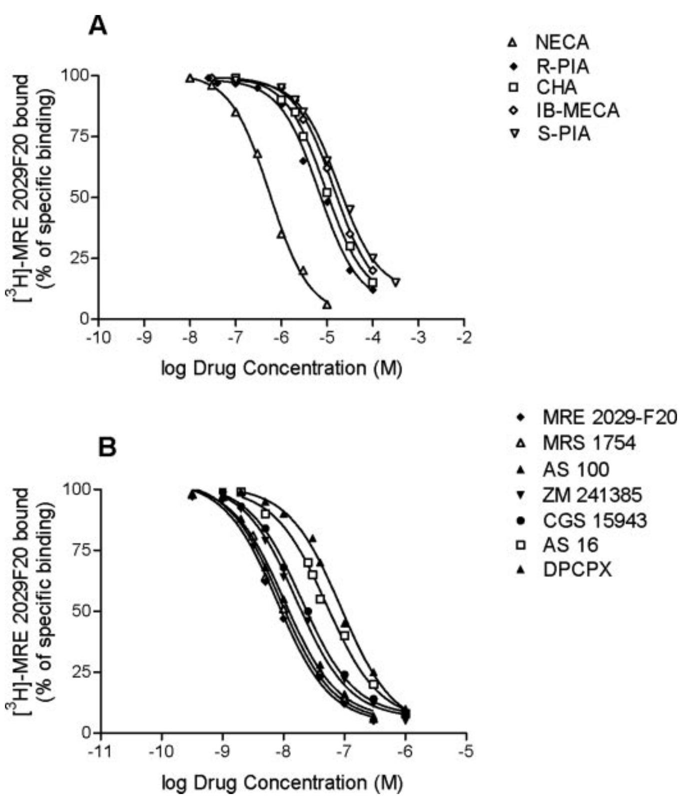

Fig. 4. Competition curves of specific [^{3}H]MRE 2029-F20 binding to human A_{2B} adenosine receptors in HEK 293 cells by adenosine agonists (A) and antagonists (B). Curves are representative of a single experiment from a series of four independent experiments. Competition experiments were preformed as described under *Materials and Methods*.

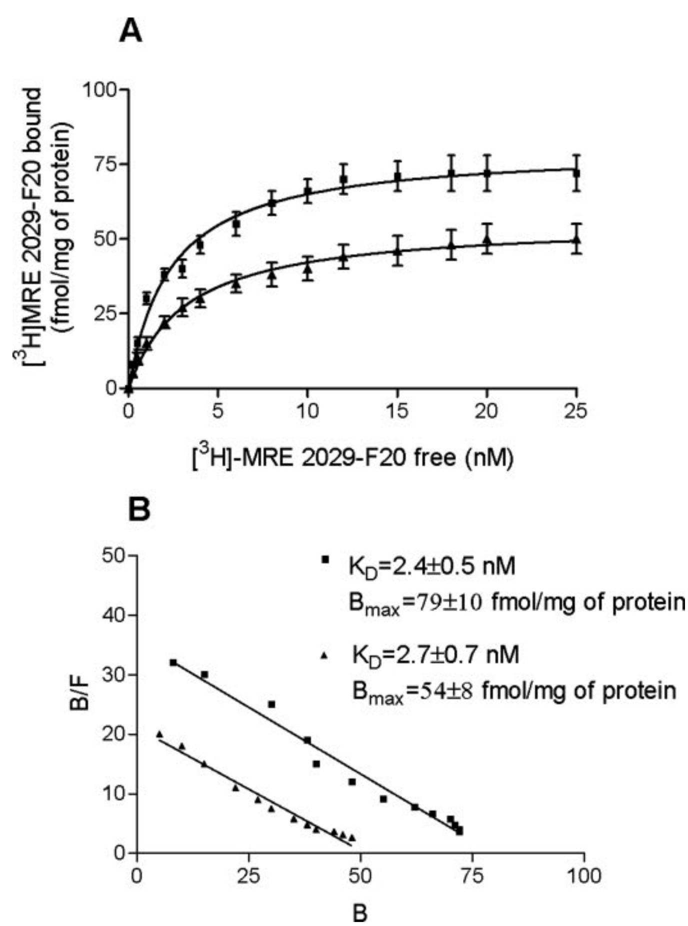

Fig. 5. A, saturation of [^{3}H]MRE 2029-F20 binding to A_{2B} adenosine receptors in human neutrophils (■) and lymphocytes (▲). B, Scatchard plots of the same data are shown. K_D values were 2.4 ± 0.5 and 2.7 ± 0.7 nM and B_{max} values were 79 ± 10 and 54 ± 8 fmol/mg of protein in neutrophils and lymphocytes, respectively. Data points are the means and vertical lines are the S.E.M. of four separate experiments performed in triplicate. Experiments were performed as described under *Materials and Methods*.

MRE 2029-F20 or 100 nM SCH 58261. In the first case, the EC_{50} values related to the A_{2A} component were 39 ± 6 and 70 ± 10 nM in neutrophils and lymphocytes, respectively. In the second condition, the EC_{50} values of NECA related to the A_{2B} receptor stimulation were 2100 ± 220 and 2640 ± 240 nM in neutrophils and lymphocytes, respectively (Fig. 7, A and B).

Phosphoinositide Turnover. It is well known that A_{2B} receptors, in addition to adenylyl cyclase, are also coupled to phospholipase C and stimulate phosphoinositide production. In hA_{2B}HEK 293 cells, 1 μM NECA induced a significant stimulation of IP_3 generation raising from basal values of 1.0 ± 0.3 to 15 ± 2 pmol of IP_3 from 1 × 10^6 cells ($P < 0.01$, $n = 3$). Pretreatment of the cells with 100 nM MRE 2029-F20 and the aminosteroid PLC inhibitor U73122 (5 μM) antagonized the NECA-mediated IP_3 generation, suggesting the involvement of A_{2B} receptors and PLCβ, respectively (Fig. 8A). When IP_3 generation was evaluated in human lymphocytes, we could not observe any coupling to PLCβ. In contrast, in human neutrophils, it was possible to detect IP_3 turnover induced by classic stimuli linked to PLC activation, such as 10 μM formyl-methionyl-leucyl phenylalanine and 100 μM NECA. This dose of NECA induced an increase from 0.45 ± 0.15 to 5.94 ± 0.5 pmol of IP_3 from 1 × 10^6 cells that was significantly reduced in the presence of 100 nM MRE 2029-F20 and 5 μM U73122 (2.5 ± 0.5 and 0.7 ± 0.2 pmol/10^6 cells, respectively) ($P < 0.01$, $n = 3$) (Fig. 8B).

Intracellular Calcium Measurements. To better characterize A_{2B} coupling to PLC activation, intracellular calcium levels were determined. NECA revealed a marked concentration-dependent increase of intracellular Ca^{2+} in hA_{2B}HEK 293 cells with an EC_{50} value of 312 ± 30 nM (Fig. 9A). This effect was potently reversed by increasing concentrations of MRE 2029-F20, showing an IC_{50} value of 12 ± 2 nM (Fig. 9B). Treatment with 5 μM U73122 completely abrogated NECA-induced calcium increase, whereas no changes in calcium levels were observed in the presence of pertussis toxin that inactivate Gi and Go family G proteins (Fig. 9C). These data suggest that A_{2B} receptors in hA_{2B}HEK 293 cells signal through the activation of $Gq_{/11}$ protein and PLCβ enzyme. To investigate the coupling of A_{2B} receptors with this pathway also in native cells, we performed the same experiments in human lymphocytes and neutrophils. Consistent with IP_3 assay, in human lymphocytes, A_{2B} receptors did not seem to stimulate intracellular calcium levels. As for human neutrophils, we observed that 100 μM NECA increases intracellular calcium levels (Fig. 10A). This effect was antagonized by MRE 2029-F20 with an IC_{50} value of 125 ± 23 nM and completely abrogated in the presence of the PLC inhibitor

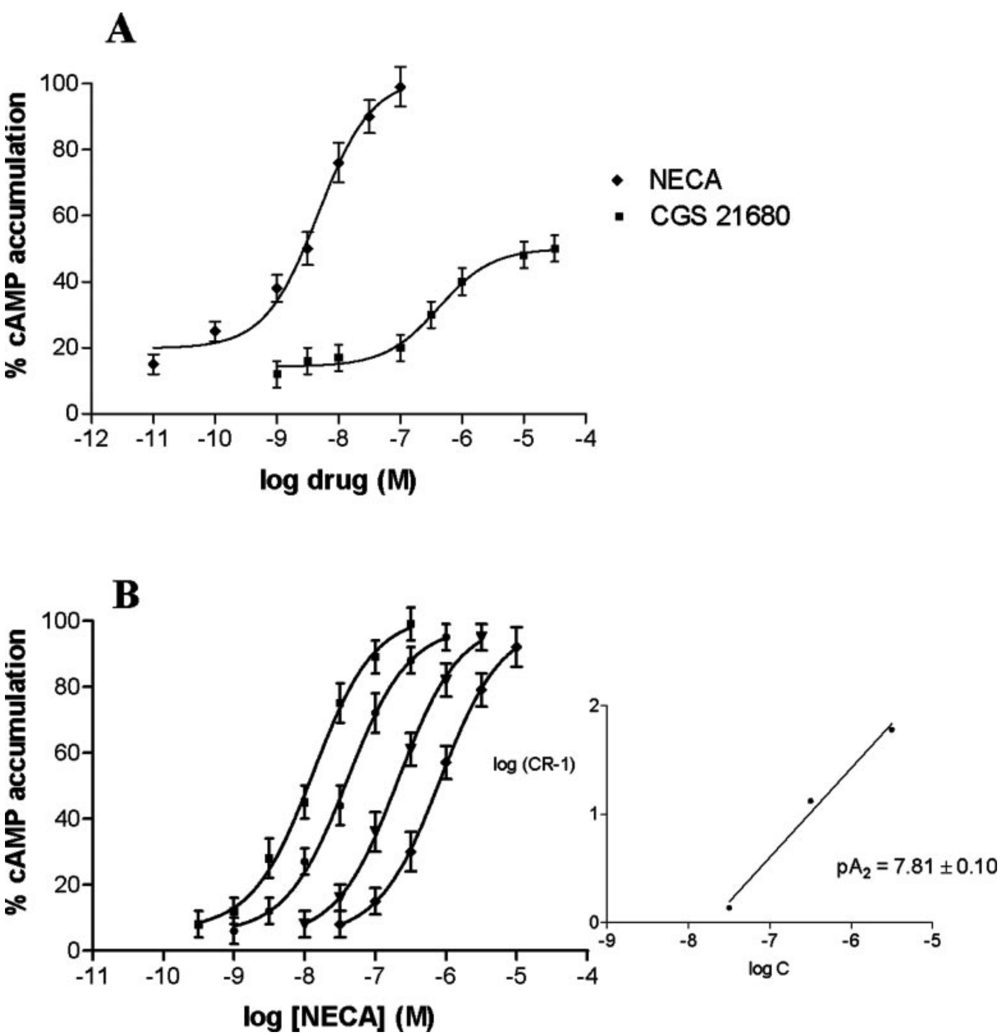

Fig. 6. A, effect of increasing concentrations of NECA and CGS 21680 on cAMP accumulation in hA_{2B}HEK 293 cells (EC_{50} = 4.5 ± 0.4 and 410 ± 52 nM, respectively). The data are normalized to the maximal NECA response. B, dose-response curves for cAMP accumulation in the absence (■) and in the presence of increasing concentrations of MRE 2029-F20 [30 nM (●), 300 nM (▼), 3000 nM (◆)] and with a fixed concentration of SCH 58261 (100 nM). The inset is a Schild plot giving a pA_2 of 7.81 ± 0.10 and a slope of 0.82 ± 0.25. C, molar concentration of MRE 2029-F20; CR, ratio of the IC_{50} values of NECA in the presence and absence of MRE 2029-F20. Results are presented as the mean ± S.E.M. of three independent experiments.

U73122 indicating the involvement of A_{2B} receptors and PLCβ enzyme (Fig. 10, A and B).

Discussion

In this work, we have compared the pharmacological behavior and the functional coupling of recombinant A_{2B} adenosine receptors expressed in transfected HEK 293 cells with endogenous receptors present in peripheral blood cells by using the novel radiolabeled receptor antagonist [^{3}H]MRE 2029-F20. In saturation assays, this radioligand shows a K_D value of 2.8 nM, in agreement with data obtained from kinetic experiments, and a receptor density of 450 fmol/mg of protein. The pharmacology of A_{2B} receptors shows that reference adenosine ligands bound to human A_{2B} receptors with a rank order of potency typical of the A_{2B} subtype. Adenosine antagonists show affinity values similar to those reported in literature. In particular, MRE 2029-F20 has affinity and selectivity values comparable with those of MRS 1754 and better than OSIP339391, ZM 241385, and DPCPX. In competition experiments performed in cells transfected with A_1, A_{2A}, and A_3 receptors, MRE 2029-F20 displayed a selectivity of 88-fold and >300-fold for A_{2B} than for A_1 (K_i value of 245 ± 31 nM), A_{2A}, and A_3 receptors (K_i > 1000 nM), respectively. Taken together, these binding characteristics make [^{3}H]MRE 2029-F20 a useful tool for detection of A_{2B} receptors, not only in transfected cells but also in native systems. [^{3}H]MRE 2029-F20 was used in this work to investigate the presence of A_{2B} receptors in peripheral blood cells chosen because 1) they represent primary cells expressing endogenous adenosine receptors; 2) they are important inflammatory cells, potentially involved in the exacerbation of asthma and other inflammation conditions; and 3) they contain more than one adenosine receptor subtype and are therefore difficult to study without the availability of selective radioligands.

First of all, the presence of A_{2B} mRNA message in lymphocytes, neutrophils, and monocytes was assessed through real-time RT-PCR assays revealing the presence of A_{2B} transcript with the following increasing rank order: monocytes < lymphocytes ≈ neutrophils. Therefore, the A_{2B} message was investigated at the protein level by using [^{3}H]MRE 2029-F20 binding, which shows a single class of high-affinity binding sites with K_D values of 2.4 ± 0.5 and 2.7 ± 0.7 nM and B_{max} values of 79 ± 10 and 54 ± 8 fmol/mg of protein in neutrophils and lymphocytes, respectively. The pharmacological profile of A_{2B} ligands in these cells confirmed the data obtained in transfected hA_{2B}HEK 293 cells; MRE 2029-F20 was the most potent compound followed by MRS 1754, AS 100, ZM 241385, and DPCPX. As for agonists, they all confirm a low affinity for the A_{2B} site. In contrast to mRNA presence of A_{2B} receptors, in human monocytes it was not possible to detect any specific binding of [^{3}H]MRE 2029-F20, and this is in agreement to findings reported by Thiele et al. (2004) showing an increase of A_{2B} message in cultured human monocytes in comparison with freshly isolated cells but not A_{2B} receptor functionality.

In 1999, Linden et al. reported that in transfected HEK 293 cells, A_{2B} receptors seem to be coupled to adenylyl cyclase and phospholipase C activity; in the same work, coupling to Gq proteins was also observed in HMC-1 cells. However, it is well known that recombinant receptors that are expressed in very high concentrations may produce different coupling in comparison with natural systems in which they are present at a lower level. Therefore, we

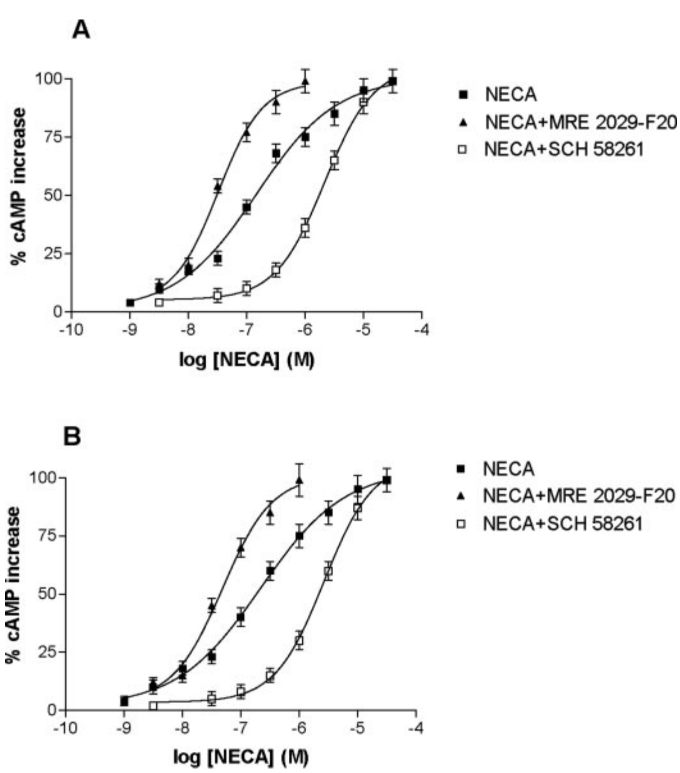

Fig. 7. A, effect of increasing concentrations of NECA alone (■) and in the presence of a fixed concentration (100 nM) of SCH 58261 (□) or MRE 2029-F20 (▲) on cAMP accumulation in human neutrophils (EC_{50} = 147 ± 16, 2100 ± 220, and 39 ± 6 nM, respectively). B, effect of increasing concentrations of NECA alone (■) and in the presence of a fixed concentration of SCH 58261 (□) or MRE 2029-F20 (▲) on cAMP accumulation in human lymphocytes (EC_{50} = 220 ± 20, 2640 ± 240, and 70 ± 10 nM, respectively). 100% represents the percentage maximal response for each curve. Results are presented as the mean ± S.E.M. of five independent experiments.

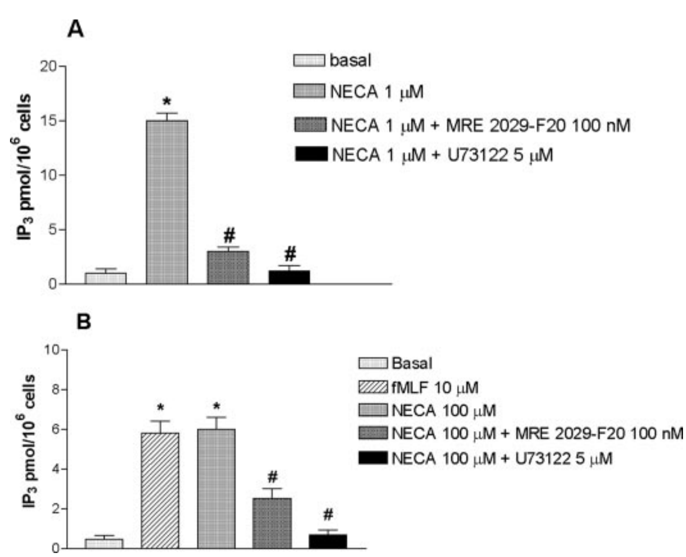

Fig. 8. A, effect of 1 μM NECA on IP_3 production in hA_{2B}HEK 293 cells and antagonism by 100 nM MRE 2029-F20 and 5 μM U73122. B, effect of 10 μM fMLF (added for 30 s) and 100 μM NECA (added for 30 min) on IP_3 production in human neutrophils and antagonism by 100 nM MRE 2029-F20 and 5 μM U73122. Results are presented as the mean ± S.E.M. of three independent experiments. (Student's t test; *, P < 0.01 versus basal; #, P < 0.01 versus NECA).

compared the intracellular signaling pathways regulated by A_{2B} adenosine receptors in both recombinant systems and native cells. To achieve this, we investigated the

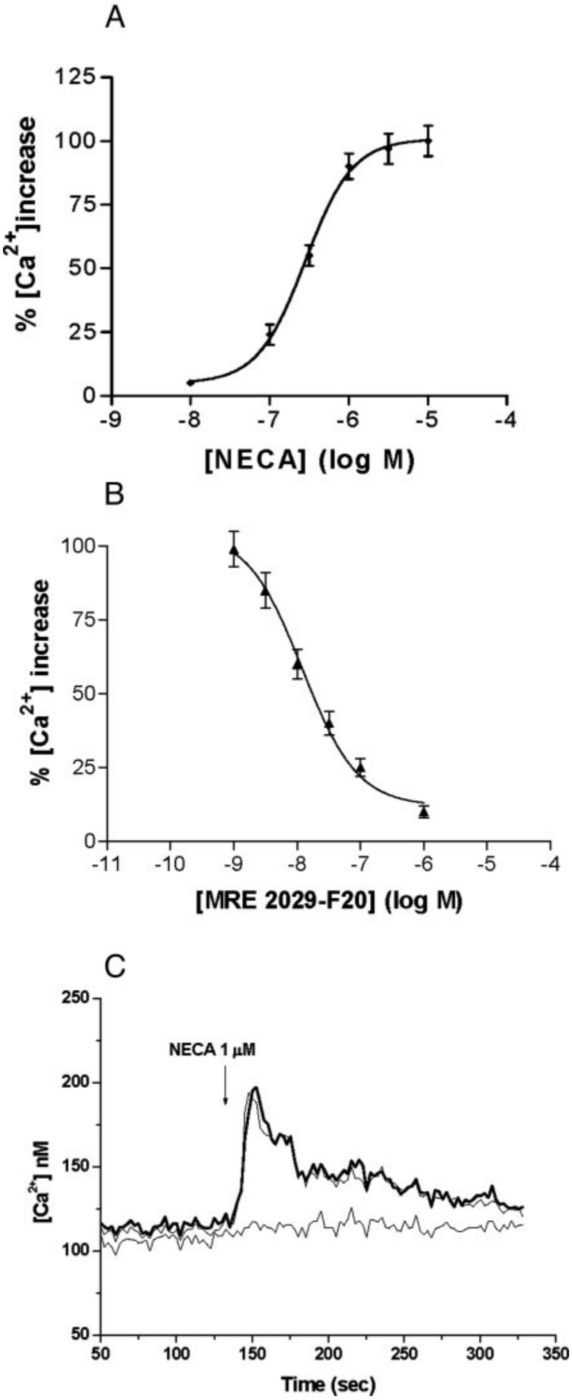

Fig. 9. A, effect of increasing concentrations of NECA on intracellular Ca^{2+} levels in hA_{2B}HEK 293 cells (EC_{50} = 312 ± 30 nM). $[Ca^{2+}]_i$ was monitored at 37°C with Fura-2 in hA_{2B}HEK 293 cells. Responses were measured relative to the peak response to 10 μM NECA. Forty-fifty cells were analyzed in each experiment. The results are typical of four experiments. B, antagonism by MRE 2029-F20, added 10 min before agonist, on the 500 nM NECA-induced stimulation of calcium release in hA_{2B}HEK 293 cells (IC_{50} = 12 ± 2 nM). C, typical traces that visualize stimulation of intracellular Ca^{2+} levels in hA_{2B}HEK 293 cells by 1 μM NECA in the absence and in the presence of PTX (200 ng/ml for 18 h) (top traces, bold and light, respectively) and effect of U73122 5 μM (bottom trace). The results are typical of four experiments.

regulation of adenylyl cyclase and phospholipase C activity by A_{2B} receptors, using NECA as the most potent nonselective A_{2B} agonist available and MRE 2029-F20 as a highly selective A_{2B} antagonist in HEK 293 cells, neutrophils, and lymphocytes. It is interesting that in the cAMP accumulation assay, NECA exhibited a potency higher than that observed in binding experiments, according to Linden et al. (1999). Because this effect was not potently reversed by MRE 2029-F20 (IC_{50}, 150 nM), we investigated the possible presence of A_{2A} receptors in these cells. Even though previous studies reported the absence of A_{2A} transcript and protein in HEK 293 cells (Cooper et al., 1997; Gao et al., 1999), in our conditions, real-time RT-PCR and binding studies revealed the presence of A_{2A} receptors (B_{max} of 35 fmol/mg of protein). Therefore, new experiments to determine the potency of MRE 2029-F20 to counteract the NECA-induced cAMP levels were performed in the presence of a fixed concentration of the A_{2A} blocker SCH 58261. With this experimental approach, the A_{2B} antagonist showed a pA_2 of 7.8, which was consistent with its binding affinity. The discrepancy between our data and previous data might be related either to a different method used to reveal A_{2A} receptors or to a different strain

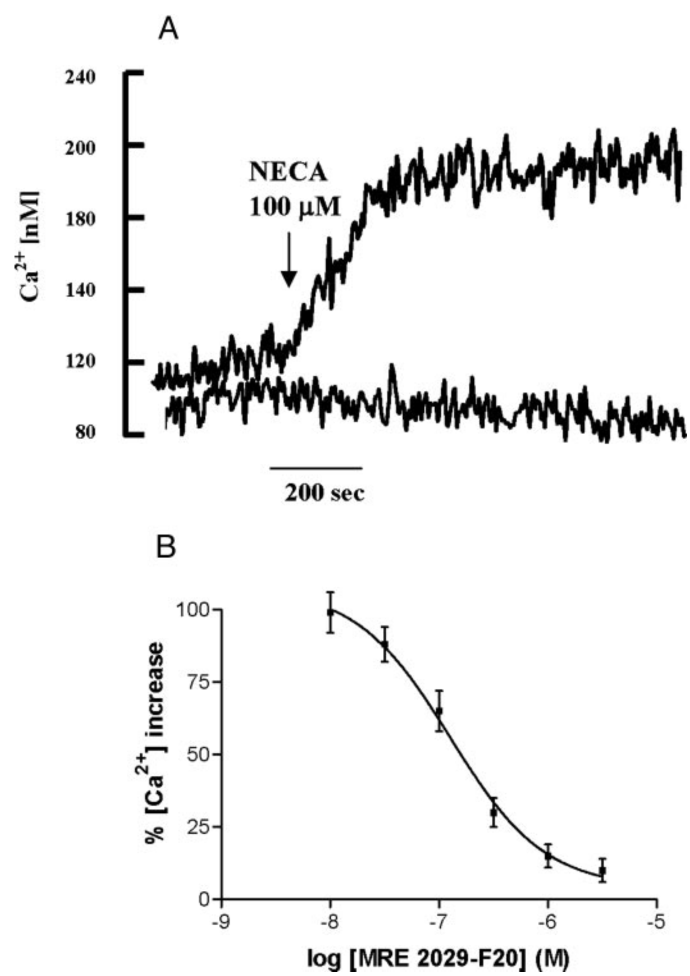

Fig. 10. A, effect of 100 μM NECA, on intracellular Ca^{2+} levels in human neutrophils in the absence (top trace) and in the presence (bottom trace) of U73122 5 μM. B, antagonism by MRE 2029-F20 on the 100 μM NECA-stimulated intracellular calcium levels in human neutrophils. The IC_{50} value was calculated to be 125 ± 23 nM. The results are typical of four experiments.

of HEK 293 cells. In native cells, the coexpression of all adenosine subtypes coupled to the same effector system makes it impossible to study the contribution of each receptor subtype without the availability of selective ligands. Because of the lack of selectivity of NECA, cAMP accumulation in peripheral blood cells was evaluated by using the same pharmacological approach described above and previously reported in HMC-1 cells (Feoktistov and Biaggioni, 1998). The stimulatory effect on cAMP levels caused by the A_{2A} receptor was distinguished from an A_{2B} effect through the use of SCH 58261 and MRE 2029-F20 as A_{2A} and A_{2B} selective antagonists, respectively. Functional A_1 and A_3 subtypes are also present together with A_{2A} and A_{2B} in both neutrophils and lymphocytes (Gessi et al., 2002, 2004). In most cases, a selective blockade of inhibitory adenosine receptors is required to unmask functional stimulatory subtypes (Feoktistov and Biaggioni, 1997). However, under our conditions, as already reported in various glial cells (Fiebich et al., 1996), it was not necessary to block A_1 and A_3 receptors to observe either A_{2A} or A_{2B} cAMP stimulation. The simultaneous expression of different adenosine subtypes in a single cell is more of a rule than an exception. Because A_{2B} receptors have low affinity for adenosine it is possible that their role become important in pathologic conditions, when adenosine levels increase. However it has to be noted that other intracellular signaling pathways have been associated with the A_{2B} stimulation.

In agreement with literature data showing A_{2B}/Gq coupling in a variety of cells (Feoktistov and Biaggioni, 1995; Strohmeier et al., 1995; Linden et al., 1998, 1999; Gao et al., 1999; Grant et al., 2001; Feoktistov et al., 2002; Rees et al., 2003), we also found that A_{2B} receptors in hA_{2B}HEK 293 cells activate PLCβ, as demonstrated by inositol phosphate generation and calcium mobilization experiments. NECA induced a significant increase in IP_3 production that was counteracted by the A_{2B} antagonist MRE 2029-F20 and also by the PLC inhibitor U73122. In calcium mobilization studies, NECA had an EC_{50} in the high nanomolar range, in agreement with its affinity in binding experiments, and MRE 2029-F20 was able to potently antagonize this effect. A_{2B} regulation of intracellular calcium increase was dependent on $G_{q/11}$ and PLCβ as demonstrated in experiments carried out in the presence of pertussis toxin and U73122. Stimulation of intracellular calcium levels was not observed in wild-type HEK 293 cells, according to Ryzhov et al. (2004), but in contrast with Gao et al. (1999). Again, a different strain of cells might be responsible for these discrepancies, and under our experimental conditions, one could hypothesize that the increase in levels of receptor expression obtained by transfection technique led to a gain in coupling of A_{2B} receptors to PLC signaling pathway. As for neutrophils, both IP_3 production and calcium increase were observed after 100 μM NECA stimulation. Because of the presence of A_3 receptors in human neutrophils that might be coupled to PLC (Gessi et al., 2002), we verified the role of A_{2B} receptors in the NECA-induced effect. MRE 2029-F20 reduced both IP_3 production and intracellular calcium increase, showing a potency in the nanomolar range that was consistent with the involvement of the A_{2B} subtype. The coupling to PLCβ was not observed in human lymphocytes (Mirabet et al., 1999), where the amount of A_{2B} receptors was slightly lower compared with human neutrophils, suggesting that receptor density might be important to establish the signaling pathways activated by receptor agonist stimulation.

In conclusion, in this work, we have demonstrated the presence and functional coupling of human A_{2B} adenosine receptors in different peripheral blood cells that play a role in immune and inflammatory processes in which A_{2B} receptors are thought to be involved. This analysis was made possible by [^{3}H]MRE 2029-F20, a new selective and high-affinity antagonist radioligand for human A_{2B} adenosine receptors that has been successfully employed to detect and quantify the amount of this adenosine subtype in native cells. Our data reveal that recombinant A_{2B} receptors expressed in HEK 293 cells show binding characteristics similar to those presented by A_{2B} subtypes expressed in peripheral blood cells but might differ from these in terms of signal transduction coupling as seen in lymphocytes. Further studies might elucidate other effects mediated by A_{2B} receptors in neutrophils and lymphocytes, such as their involvement in superoxide anion generation or in cytokine release. The appreciation of the pathways activated by A_{2B} receptors in native cells raises the possibility that selective antagonists may become useful tools for the pharmacological characterization of diseases in which A_{2B} receptors may be involved and possibly a basis for drug development.

References

Abo-Salem OM, Hayallah AM, Bilkei-Gorzo A, Filipek B, Zimmer A, and Muller CE (2004) Antinociceptive effects of novel A_{2B} adenosine receptor antagonists. *J Pharmacol Exp Ther* **308:**358–366.

Afzal A, Shaw LC, Caballero S, Spoerri PE, Lewin AS, Zeng D, Belardinelli L, and Grant MB (2003) Reduction in preretinal neovascularization by ribozymes that cleave the A_{2B} adenosine receptor mRNA. *Circ Res* **93:**500–506.

Baraldi PG, Tabrizi MA, Preti D, Bovero A, Fruttarolo F, Romagnoli R, Moorman AR, Gessi S, Merighi S, Varani K, et al. (2004a) [^{3}H]MRE 2029-F20, a selective antagonist radioligand for the human A_{2B} adenosine receptors. *Bioorg Med Chem Lett* **14:**3607–3610.

Baraldi PG, Tabrizi MA, Preti D, Bovero A, Romagnoli R, Fruttarolo F, Zaid NA, Moorman AR, Varani K, Gessi S, et al. (2004b) Design, synthesis and biological evaluation of new 8-heterocyclic xanthine derivatives as highly potent and selective human A_{2B} adenosine receptor antagonists. *J Med Chem* **47:**1434–1447.

Borea PA, Dalpiaz A, Varani K, Gessi S, and Gilli G (1996) Binding thermodynamics at A_1 and A_{2A} adenosine receptors. *Life Sci* **59:**1373–1388.

Bradford MM (1976) A rapid and sensitive method for the quantification of microgram quantities of protein utilizing the principle of protein dye-binding. *Anal Biochem* **72:**248–254.

Challiss RA, Chilvers ER, Willcocks AL, and Nahorski SR (1990) Heterogeneity of [^{3}H]inositol 1,4,5-trisphosphate binding sites in adrenal-cortical membranes. Characterization and validation of a radioreceptor assay. *Biochem J* **265:**421–427.

Chen C and Okayama H (1987) High-efficiency transformation of mammalian cells by plasmid DNA. *Mol Cell Biol* **7:**2745–2752.

Chomczynski P and Sacchi N (1987) Single-step method of RNA isolation by acid guanidinium thiocyanate-phenol-chloroform extraction. *Anal Biochem* **162:**156–159.

Cooper J, Hill SJ, and Alexander SP (1997) An endogenous A_{2B} adenosine receptor coupled to cyclic AMP generation in human embryonic kidney (HEK 293) cells. *Br J Pharmacol* **122:**546–550.

Feoktistov I and Biaggioni I (1995) Adenosine A_{2B} receptors evoke interleukin-8 secretion in human mast cells. An enprofylline-sensitive mechanism with implications for asthma. *J Clin Investig* **96:**1979–1986.

Feoktistov I and Biaggioni I (1997) Adenosine A_{2B} receptors. *Pharmacol Rev* **49:**381–402.

Feoktistov I and Biaggioni I (1998) Pharmacological characterization of adenosine A_{2B} receptors: studies in human mast cells co-expressing A_{2A} and A_{2B} adenosine receptor subtypes. *Biochem Pharmacol* **55:**627–633.

Feoktistov I, Garland EM, Goldstein AE, Zeng D, Belardinelli L, Wells JN, and Biaggioni I (2001) Inhibition of human mast cell activation with the novel selective adenosine A2B receptor antagonist 3-isobutyl-8-pyrrolidinoxanthine (IPDX). *Biochem Pharmacol* **62:**1163–1173.

Feoktistov I, Goldstein AE, Ryzhov S, Zeng D, Belardinelli L, Voyno-Yasenetskaya T, and Biaggioni I (2002) Differential expression of adenosine receptors in human endothelial cells: role of A_{2B} receptors in angiogenic factor regulation. *Circ Res* **90:**531–538.

Feoktistov I, Ryzhov S, Goldstein AE, and Biaggioni I (2003) Mast cell-mediated stimulation of angiogenesis: cooperative interaction between A_{2B} and A_3 adenosine receptors. *Circ Res* **92:**485–492.

Fiebich BL, Biber K, Gyufko K, Berger M, Bauer J, and van Calker D (1996)

Adenosine A_{2B} receptors mediate an increase in interleukin (IL)-6 mRNA and IL-6 protein synthesis in human astroglioma cells. *J Neurochem* **66:**1426–1431.

Fredholm BB (2003) Adenosine receptors as targets for drug development. *Drug News Perspect* **16:**283–289.

Fredholm BB, IJzerman AP, Jacobson KA, Klotz KN, and Linden J (2001) International Union of Pharmacology. XXV. Nomenclature and classification of adenosine receptors. *Pharmacol Rev* **53:**527–552.

Gao Z, Chen T, Weber MJ, and Linden J (1999) A_{2B} adenosine and P2Y2 receptors stimulate mitogen-activated protein kinase in human embryonic kidney-293 cells. *J Biol Chem* **274:**5972–5980.

Gessi S, Varani K, Merighi S, Cattabriga E, Avitabile A, Gavioli R, Fortini C, Leung E, Mac Lennan S, and Borea PA (2004) Expression of A_3 adenosine receptors in human lymphocytes: up-regulation in T cell activation. *Mol Pharmacol* **65:**711–719.

Gessi S, Varani K, Merighi S, Cattabriga E, Iannotta V, Leung E, Baraldi PG, and Borea PA (2002) A_3 adenosine receptors in human neutrophils and promyelocytic HL60 cells: a pharmacological and biochemical study. *Mol Pharmacol* **61:**415–424.

Grant MB, Davis MI, Caballero S, Feoktistov I, Biaggioni I, and Belardinelli L (2001) Proliferation, migration and ERK activation in human retinal endothelial cells through A_{2B} adenosine receptor stimulation. *Investig Ophtal Vis Sci* **42:**2068–2073.

Higuchi R, Fockler C, Dollinger G, and Watson R (1993) Kinetic PCR analysis: real-time monitoring of DNA amplification reactions. *Biotechnology* **11:**1026–1030.

Ji X, Kim YC, Ahern DG, Linden J, and Jacobson KA (2001) [^{3}H]MRS 1754, a selective antagonist radioligand for A(2B) adenosine receptors. *Biochem Pharmacol* **61:**657–663.

Linden J, Auchampach JA, Jin X, and Figler RA (1998) The structure and function of A_1 and A_{2B} adenosine receptors. *Life Sci* **62:**1519–1524.

Linden J, Thai T, Figler H, Jin X, and Robeva A (1999) Characterization of human A_{2B} adenosine receptors: radioligand binding, western blotting and coupling to Gq in human embryonic kidney 293 cells and HMC-1 mast cells. *Mol Pharmacol* **56:**705–713.

Livingston M, Heaney LG, and Ennis M (2004) Adenosine, inflammation and asthma- a review. *Inflamm Res* **53:**171–178.

Mirabet M, Herrera C, Cordero OJ, Mallol J, Lluis C, and Franco R (1999) Expression of A_{2B} adenosine receptors in human lymphocytes: their role in T cell activation. *J Cell Sci* **112:**491–502.

Munson PJ and Rodbard D (1980) Ligand: a versatile computerized approach for the characterization of ligand binding systems. *Anal Biochem* **107:**220–239.

Rees DA, Lewis BM, lewis MD, Francis K, Scanlon MF, and Ham J (2003) Adenosine-induced IL-6 expression in pituitary folliculostellate cells is mediated via A_{2B} adenosine receptors coupled to PKC and p38 MAPK. *Br J Pharmacol* **140:**764–772.

Rivkees SA and Reppert SM (1992) RFL9 encodes an A2B-adenosine receptor. *Mol Endocrinol* **6:**1598–1604.

Ryzhov S, Goldstein A, Matafonov A, Feoktistov I, and Biaggioni I (2004) Migration of adenosine A_{2B} receptors to low density membrane fractions and coupling to phospholipase C, in *Abstract Book, 4th International Symposium of Nucleosides and Nucleotides*; 2004 Jun 6–9; Chapel Hill, NC. pp 70, abstr. 71M. http://www.purines.org/Purines2004_AbstractBook.pdf

Stewart M, Steinig AG, Ma C, Song JP, McKibben B, Castelhano AL, and MacLennan SJ (2004) [^{3}H]OSIP339391, a selective, novel and high affinity antagonist radioligand for adenosine A_{2B} receptors. *Biochem Pharmacol* **68:**305–312.

Strohmeier GR, Reppert SM, Lencer WI, and Madara JL (1995) The A_{2B} adenosine receptor mediates cAMP responses to adenosine receptor agonists in human intestinal epithelia. *J Biol Chem* **270:**2387–2394.

Talukder MA, Morrison RR, Ledent C, and Mustafa SJ (2003) Endogenous adenosine increases coronary flow by activation of both A_{2A} and A_{2B} receptors in mice. *J Cardiovasc Pharmacol* **41:**562–570.

Thiele A, Kronstein R, Wetzel A, Gerth A, Nieber K, and Hauschildt S (2004) regulation of adenosine receptor subtypes during cultivation of human monocytes: role of receptors in preventing lipopolysaccharide-triggered respiratory burst. *Infect Immun* **72:**1349–1357.

Varani K, Merighi S, Gessi S, Klotz KN, Leung E, Baraldi PG, Cacciari B, Romagnoli R, Spalluto G, and Borea PA (2000) [^{3}H]MRE 3008F20: a novel antagonist radioligand for the pharmacological and biochemical characterization of human A_3 adenosine receptors. *Mol Pharmacol* **57:**968–975.

Varani K, Gessi S, Dalpiaz A, Ongini E, and Borea PA (1997) Characterization of A_{2A} adenosine receptors in human lymphocyte membranes by [^{3}H]SCH 58261 binding. *Br J Pharmacol* **122:**386–392.

Zhong H, Belardinelli L, Maa T, Feoktistov I, Biaggioni I, and Zeng D (2004) A_{2B} adenosine receptors increase cytokine release by bronchial smooth muscle cells. *Am J Respir Cell Mol Biol* **30:**118–125.

Address correspondence to: Prof. Dr. Pier Andrea Borea, Chair of Pharmacology, Faculty of Medicine, University of Ferrara, Department of Clinical and Experimental Medicine, Pharmacology Unit, Via Fossato di Mortara 17-19, 44100 Ferrara, Italy. E-mail: bpa@dns.unife.it